Chemical Trends in the Near-Edge X-ray Absorption Fine Structure of Monosubstituted and Para-Bisubstituted Benzenes

Ryan R. Cooney and Stephen G. Urquhart*

Department of Chemistry, University of Saskatchewan, Saskatoon, Saskatchewan S7N 5C9, Canada

Received: July 14, 2004; In Final Form: September 2, 2004

Carbon 1s (C−R) → $\pi^*_{C=C}$ electronic transitions originating from the substituent-bonded carbon atom of a benzene ring show distinctive chemical shifts in their near-edge X-ray absorption fine structure (NEXAFS) spectra. We have systematically explored these chemical shifts through ab initio calculations and carefully calibrated experimental data for a wide range of molecules containing substituted benzene rings. The systematic disparity between experimental and calculated transition energies was used to develop a semiempirical correction for this class of transitions, allowing us to map calculated transition energies onto a corrected, experimental energy scale. The correction method was applied to a large set of calculated core C 1s (C−R) → $\pi^*_{C=C}$ transition energies, and used to prepare a chemically wide-ranging NEXAFS correlation diagram for the "C−R π^* band". We demonstrate the usefulness of this correlation diagram for the analytical application of NEXAFS spectroscopy and microscopy to organic materials.

1. Introduction

Near-edge X-ray absorption fine structure (NEXAFS) spectroscopy, in tandem with X-ray microscopy, can be used to characterize the chemical composition of organic materials at spatial scales as fine as 30 nm.[1] Recent applications of NEXAFS spectroscopy and microscopy include the chemical characterization of polymers,[1−5] the chemical analysis of surfaces,[6−10] and thin films of relevance to semiconductors and devices.[11,12]

In applications of NEXAFS microscopy to organic materials, the narrow carbon 1s → π^* transitions often have the greatest analytic utility due to their narrow energy width and their chemical sensitivity.[3,7,9,13,14] Previously, the chemical sensitivity of the carbonyl C 1s and O 1s (C═O) → $\pi^*_{C=O}$ transitions had been illustrated by examining a series of polymers containing the carbonyl functionality in a variety of different bonding environments.[15] A 3.8-eV range in the C 1s (C═O) → $\pi^*_{C=O}$ transition energy was observed, and explained through the use of ab initio calculations. The discrepancies between the calculated and the experimental transition energies were shown to be systematic, allowing for a semiempirical correction of the transition energy. From this, a comprehensive correlation diagram for NEXAFS spectroscopy was developed.

The carbon 1s (C−R) → $\pi^*_{C=C}$ transitions of substituted benzene compounds have a similar chemical sensitivity. Benzene compounds show a narrow absorption band at ∼285 eV from the C 1s (C−H) → $\pi^*_{C=C}$ transitions that originate from the "C−H" carbon atom sites on the ring. In addition to this, weaker yet distinctive C 1s → $\pi^*_{C=C}$ excitations are often seen at higher energy, between 285 and 288 eV. These features originate from a chemical shift induced by the bonding of a substituent to the benzene ring, and concurrent changes in the valence electronic structure. These transitions are often described as C 1s (C−R) → $\pi^*_{C=C}$ transitions, where "C−R" refers to the carbon at which substitution of the benzene ring occurs. These general attributes are illustrated by the NEXAFS of three aromatic polymers in Figure 1,[15] where the "C−R" peak (identified by an asterisk) shifts in energy between polycarbonate, polyurethane, and polyurea.

The "C−R" chemical shift in NEXAFS spectroscopy has useful chemical sensitivity, and has been employed, for example, to differentiate between urea and urethane linkages in macrophase separation in polyurethanes[2,3,16] and between polystyrene and poly(*p*-bromostyrene) in dewetting polymer thin films.[17] In this work, we systematically explore the chemical sensitivity of the benzene C 1s (C−R) → $\pi^*_{C=C}$ transition through ab initio calculations for a wide assortment of functionalized benzene compounds. These calculations will be compared to previously documented and well-calibrated NEXAFS or Inner Shell Electron Energy Loss (ISEELS) spectra, to establish a semiempirical method for determining the absolute (experimental) transition energy from the calculated energies. A spectroscopic correlation diagram will be developed for these "π^* C−R" transitions, and the limitations of this diagram discussed.

2. Computational Methods

Ab initio calculations were performed for a variety of substituted benzene compounds, identified in Chart 1. The molecules are organized into seven categories (halogen, oxygen, nitrogen, sulfur, carbon, carbonyl, and other functionalities) by the identity of the moiety of the "R" substituent immediately adjacent to the benzene ring. We have included singly substituted benzene groups and para-bisubstituted benzene groups. Chemical shifts due to bisubstitution patterns on benzene rings (e.g. ortho, meta, para) can be complex (see ref 18) and are beyond the scope of this paper. Excitation energies, C 1s ionization potentials, term values and oscillator strengths for the core C 1s(C−R) → $\pi^*_{C=C}$ transitions were determined with Kosugi's GSCF3 package.[19] The basis of these calculations is the improved virtual orbital approximation (IVO), proposed by Hunt and Goddard,[20] which explicitly compensates for the effect of the induced core hole in absorption processes by calculating the virtual electronic states relative to the appropriate core

* Address correspondence to this author. Fax: (306)-966-4730. E-mail: stephen.urquhart@usask.ca.

10.1021/jp046868j CCC: $27.50
Published on Web 10/30/2004

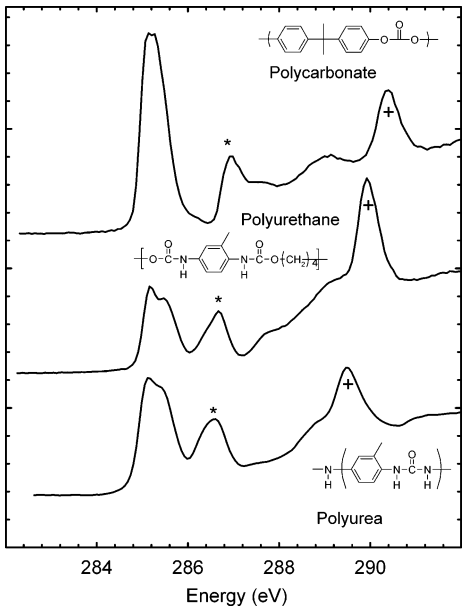

Figure 1. C 1s near-edge X-ray absorption fine structure (NEXAFS) of polycarbonate, polyurethane, and polyurea, reproduced with permission from ref 15. An asterisk identifies the C 1s (C−R) → $\pi^*_{C=C}$ transitions, and a "+" identifies the C 1s (C═O) → $\pi^*_{C=O}$ transitions.

TABLE 1: Experimental Excitation Energies for the C 1s (C−R) → $\pi^*_{C=C}$ Transition of Substituted Benzene Compounds

molecule	transition energy (eV)
fluorobenzene	287.5[33]
benzene-1,4-diol	287.25[26]
phenol	287.1[26]
anisole	287.05[32,34]
phenylamine	286.9[35]
methylphenylamine	286.8[32,36]
N-phenyl ethyl carbamate	286.7[37,38]
N-phenyl urea	286.4[37,38]
chlorobenzene	286.3[33]
bromobenzene	286.0[33]
benzonitrile	285.57[32]
dimethyl terephthalate	284.8[18]
benzaldehyde[a]	286.0[25]
benzoic acid ethyl ester[a]	287.5[25]
terephthalaldehyde[a]	285.8[25]

[a] The energy for these transitions has been reassigned (see text).

excited cation. The Hartree−Fock Hamiltonian used in the GSCF3 package is highly optimized for the calculation of core-excited states.[19]

The molecular geometries used in GSCF3 calculations were the lowest energy conformations determined with '02 Spartan ES ab initio calculations at the 6-31G* level.[21] The GSCF3 calculations were then performed with the Guassian-type extended basis set of Huzinaga et al.[22] (621/41) contracted Guassian-type functions were used on nitrogen, fluorine, and carbon atoms, (41) was applied to hydrogen, (42121/411) to oxygen, (5321/31121) to sulfur, (312121/3121) to chlorine, and (31212121/312121/31) to bromine. A higher quality basis set (411121/3111/*) was used on the core exited carbon atom. This basis set is simple enough to be applied to larger molecules while still generating high-quality NEXAFS spectral predictions. Except for indicated exceptions, only data for the C 1s(C−R) → $\pi^*_{C=C}$ transitions are presented.

3. Results and Discussions

NEXAFS Spectra of Substituted Benzene Compounds. The experimental data for the C 1s (C−R) → $\pi^*_{C=C}$ transitions are listed in Table 1 and the chemical structures for these molecules appear in Chart 1. In this compilation we have restricted our choices to NEXAFS or ISEELS spectra that have been carefully calibrated by a gas whose absolute energy scale has been accurately measured.[23] The range in energy for the C 1s (C−R) → $\pi^*_{C=C}$ transition is 2.83 eV between fluorobenzene and terephthalaldehyde. The "C−R" chemical shift can be qualita-

CHART 1: Molecular Structures of Functionalized Benzene Compounds

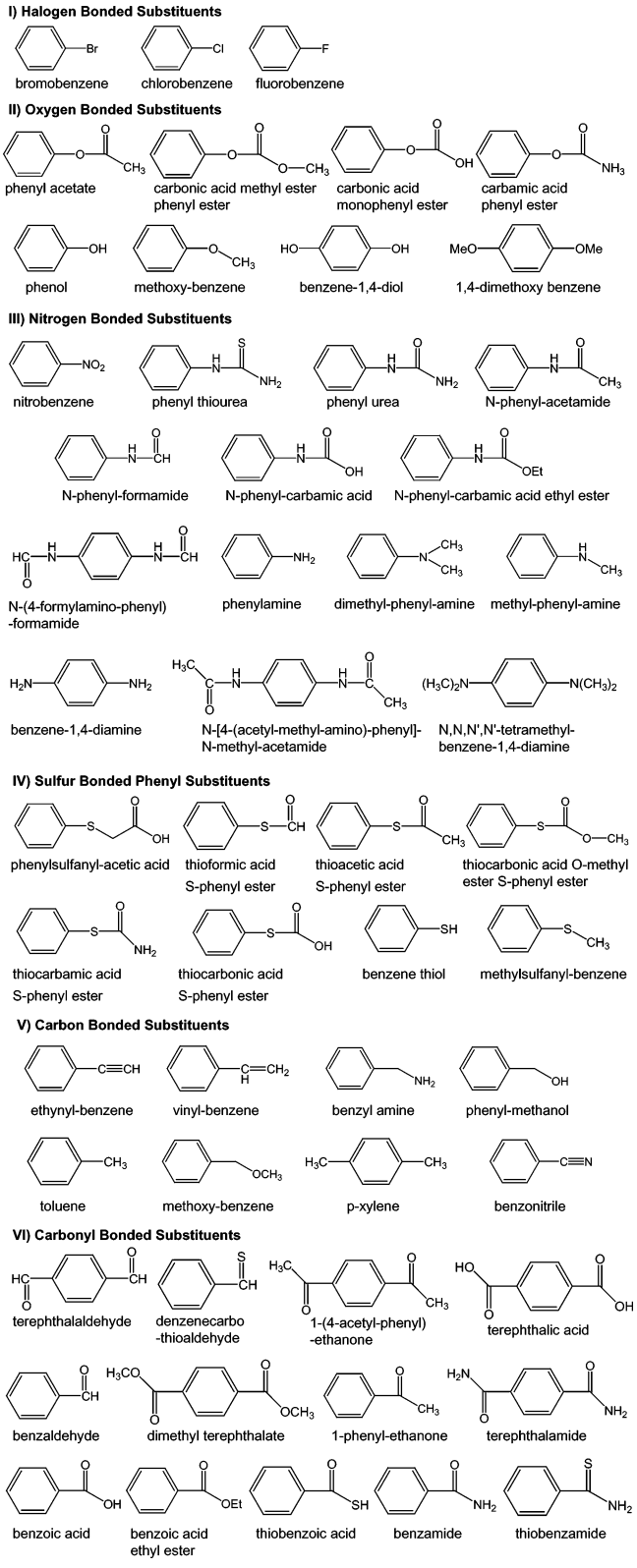

TABLE 2: Calculated Ionization Potentials for C 1s (C−R) Core Excitation, and Term Values, Transition Energies, and Oscillator Strengths for C 1s (C−R) → $\pi^*_{C=C}$ Transitions in Molecules Containing Substituted Benzene Compounds

molecule	IP (eV)	TV (eV)	energy (eV)	osc.
halogen substituents				
bromobenzene	291.81	3.38	288.43	0.0244
chlorobenzene	292.21	3.56	288.65	0.0244
fluorobenzene	293.43	3.72	289.71	0.0250
oxygen substituents				
phenyl acetate	292.74	3.77	288.97	0.0246
carbonic acid methyl ester phenyl ester	292.52	3.49	289.03	0.0241
carbonic acid monophenyl ester	292.70	3.66	289.04	0.0238
carbamic acid phenyl ester	292.47	3.40	289.07	0.0241
phenol	292.53	3.30	289.23	0.0280
methoxybenzene	292.30	3.02	289.28	0.0281
benzene-1,4-diol	292.34	2.93	289.41	0.0259
1,4-dimethoxybenzene	291.97	2.48	289.49	0.0255
nitrogen substituents				
nitrobenzene	292.80	5.05	287.75	0.0102
phenyl thiourea	292.22	3.94	288.28	0.0227
phenyl urea	292.16	3.73	288.43	0.0240
N-phenylacetamide	292.03	3.16	288.87	0.0258
N-phenylformamide	292.53	3.62	288.91	0.0269
N-phenylcarbamic acid	292.25	3.34	288.91	0.0258
N-phenyl-carbamic acid ethyl ester	292.07	3.14	288.93	0.0262
N-(4-formylaminophenyl)formamide	292.51	3.50	289.01	0.0231
phenylamine	291.89	2.86	289.03	0.0306
dimethylphenylamine	291.62	2.51	289.11	0.0301
methylphenylamine	291.87	2.69	289.18	0.0309
benzene-1,4-diamine	291.17	1.95	289.22	0.0266
N-[4-(acetylmethylamino)phenyl]-*N*-methylacetamide	292.28	3.04	289.24	0.0227
N,*N*,*N*′,*N*′-tetramethylbenzene-1,4-diamine	290.82	1.49	289.33	0.0261
sulfur substituents				
phenylsulfanylacetic acid	291.17	3.32	287.85	0.0220
thioformic acid *S*-phenyl ester	291.60	3.72	287.88	0.0220
thioacetic acid *S*-phenyl ester	290.98	3.08	287.90	0.0218
thiocarbonic acid O-methyl ester *S*-phenyl ester	291.22	3.32	287.90	0.0216
thiocarbamic acid *S*-phenyl ester	291.22	3.26	287.96	0.0213
thiocarbonic acid *S*-phenyl ester	291.61	3.62	287.99	0.0207
benzenethiol	292.38	4.29	288.09	0.0283
methylsulfanylbenzene	291.18	3.01	288.17	0.0265
carbon substituents				
ethynylbenzene	290.66	3.58	287.08	0.0205
vinylbenzene	290.79	3.44	287.35	0.0198
benzylamine	290.45	3.03	287.42	0.0243
phenylmethanol	290.58	3.10	287.48	0.0241
toluene	290.61	3.10	287.51	0.0255
methoxybenzene	290.51	3.00	287.51	0.0245
p-xylene	290.36	2.75	287.61	0.0245
benzonitrile	292.24	4.48	287.76	0.0175
carbonyl substituents				
terephthalaldehyde	291.56	4.98	286.58	0.0137
benzenecarbothioaldehyde	291.28	4.64	286.64	0.0068
1,4-diacetylbenzene	291.23	4.53	286.70	0.0149
terephthalic acid	291.71	4.87	286.84	0.0154
benzaldehyde	291.16	4.28	286.88	0.0136
dimethyl terephthalate	291.34	4.44	286.90	0.0159
1-phenylethanone	290.97	4.03	286.93	0.0152
terephthalamide	291.46	4.52	286.94	0.0172
benzoic acid	291.31	4.20	287.11	0.0148
benzoic acid ethyl ester	291.01	3.89	287.12	0.0157
thiobenzoic acid	291.33	4.20	287.13	0.0139
benzamide	291.15	4.01	287.14	0.0173
thiobenzamide	291.29	4.02	287.27	0.0151

tively correlated to the identity of the atom (or functionality) of the "R" group directly bonded to the benzene group, with the highest energy transitions generally occurring with fluorine and oxygen, and the lowest energy transitions occurring with carbon atoms and carbonyl groups, nitrogen being intermediate (i.e., F > O > N > C > (CO)).

Ab Initio Calculations. Ab initio calculations were performed to study the magnitude and the origin of the chemical shifts of the benzene core C 1s (C−R) → $\pi^*_{C=C}$ transition energy for the molecules appearing in Chart 1. The calculated excitation energies, ionization potentials, term values, and oscillator strengths are listed in Table 2. There is a large body of previous computational work for many of these species, including ab initio IVO calculations of dimethyl terephthalate,[18] *N*-phenylcarbamic ethyl ester, *N*,*N*′-diphenyl urea,[2] and *p*-xylene,[24] as well as extended Hückel MO calculations of benzaldehyde, benzoic acid ethyl ester, terephthaldehyde,[25] benzene-1,4-diol, and phenol.[26] We have repeated these calculations here with a common basis set to permit a systematic comparison of experiment to theory. Our results are similar to the previous ab initio IVO calculations, except for small differences that can be attributed to the basis set or molecular geometry. In contrast, we found substantial differences between our calculations and the previous extended Hückel MO calculations. This difference is not surprising, given the limitations of the extended Hückel method. The nature of these differences will be discussed in more detail below.

The data in Table 2 show the same trend as observed in the experimental data, that is, the dependence of the benzene C 1s (C−R) → $\pi^*_{C=C}$ transition energy on the substituent identity

(i.e., F > O > N > S > C >(CO)). The calculated ionization potentials and term values facilitate an explanation of this phenomenon. The range in this transition energy depends on the partial charge on the core excited carbon atom, as reflected by the range of 3.067 eV in the ionization potential, as well as the valence electronic structure, as reflected by the range of 3.573 eV in term values. The resulting shift in the transition energy (E = IP − TV) is 3.128 eV. In predicting the chemical shift of benzene core C 1s (C−R) → $\pi^*_{C=C}$ transitions it is imperative that both the inductive characteristics and valence electronic structure of the substituent are considered. This effect bears a similarity to the shifts observed in ^{13}C NMR spectroscopy of substituted benzenes.[27]

The higher energy C 1s(C−R) → $\pi^*_{C=C}$ transitions, from molecules containing fluorine- and oxygen-based substituents, generally have moderate term values (3.4−3.7 eV), as anticipated from the p-orbital (lone pair) character of atoms interacting with the π^* density of the benzene ring. However, the inductive characteristics of these functionalities cause the chemical shift of these transitions to be dominated by a higher ionization potential shift.

Though the large ionization potentials may be the most distinctive characteristic of C−R sites with oxygen-bound substituents, "lone pair"/benzene π^* interactions are primarily responsible for the transition energy shift for this substituent subgroup. For monosubstituted benzene species incorporating an oxygen-bound substituent, the 0.31-eV range in the C 1s(C−R) → $\pi^*_{C=C}$ transition energy arises from two opposite effects: a 0.44-eV range in ionization potentials, outweighed by the concurrent stabilization of valence electronic structure, as reflected by a 0.75-eV range in term values (see Table 2). Qualitatively, both ionization potential and term values are observed to increase as the π character of the substituent's secondary moiety is enhanced. For example, both the largest ionization potential and term value in the subgroup is recorded for phenyl acetate, where the secondary moiety is a carbonyl. Meanwhile, the smallest ionization potential and term value, in the monosubstituted series of oxygen-anchored substituents, is that of anisole, where the secondary moiety is an sp^3 carbon based methyl group. While the π^*-character has the greatest effect on the C−R transition energy within this subgroup, inductive effects must also be considered.

Not surprisingly, related trends can be observed in the subgroups with moderate inductive effects. The decrease in the C 1s(C−R) → $\pi^*_{C=C}$ transition energy, as carbon-based substiuents change from sp^3 to sp hybridization, is illustrative. This decrease is due to progressive decrease in the π^* orbital energy, as π-delocalization increases. In the intermediate nitrogen group, a distinctive species is nitrobenzene. In this case the strength of the π character induces an unusually large term value, indicating significant stabilization of the valence structure due to conjugation with the benzene ring. Generally, larger term values can be correlated with smaller oscillator strengths.

In general, transitions with a relatively small chemical shift, such as for those molecules with a carbonyl as the primary substituent bonded to the benzene ring, are characterized by larger term values (3.9−5 eV). The strong electronic interactions between the benzene π^* density and carbonyl π^* density tends to lower the transition energy and decrease the intensity of the transition. This form of benzene/carbonyl π^* conjugation has been discussed previously for substitution isomers of poly(ethylene terephthalate)[18] and polyurethanes.[2]

Correlation between Theory and Experiment. In examining the disparity between the calculated and experimental energies for the C 1s (C−R) → π^* transition, we have assembled an extensive body of calculated values, carried out at the same level of theory, and correlated them where possible to well-calibrated experimental results. Figure 2 presents the graphical relationship between calculated and measured core C 1s (C−R) → $\pi^*_{C=C}$ transition energies for a series of substituted benzene molecules; the data used in this plot are listed in Table 3. The linear correlation between the experimental and calculated values is apparent.

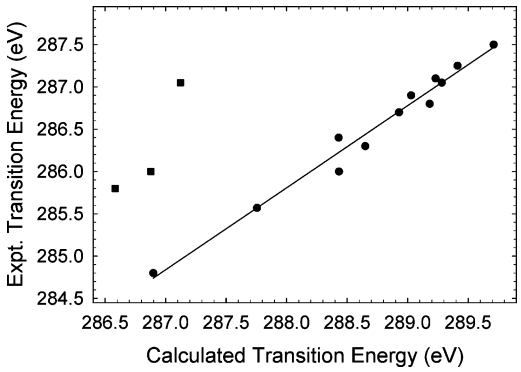

Figure 2. Linear relationship between calculated C 1s (C−R) → $\pi^*_{C=C}$ transition energies and experimental results. The squares indicate data excluded from the fit.

TABLE 3: Experimental and Calculated Excitation Energies for the C 1s (C−R) → $\pi^*_{C=C}$ Transition in Substituted Benzene Compounds

	energy (eV)	
molecule	exptl	calcd
terephthaldehyde[a]	285.8	286.58
benzaldehyde[a]	286.0	286.88
dimethyl terephthalate	284.8	286.90
benzoic acid ethyl ester[a]	287.05	287.12
benzonitrile	285.57	287.76
bromobenzene	286.0	288.43
phenyl urea	286.4	288.43
chlorobenzene	286.3	288.65
N-phenyl carbamic acid ethyl ester	286.7	288.93
phenylamine	286.9	289.03
methylphenylamine	286.8	289.18
phenol	287.1	289.23
methoxybenzene	287.05	289.28
benzene-1,4-diol	287.25	289.41
fluorobenzene	287.5	289.71

[a] These data have been excluded from the fit (see text).

As observed elsewhere, the calculated transition energies are higher than the experimental transition energies. The reason for this effect is the overscreening of the core hole in these calculations. When a core electron (in an N-electron molecule) is excited to a optical orbital of valence character, repulsion by this excited electron will perturb the rest of the molecule, e.g. the (N− 1)-electron part of the electronic structure. This perturbation will decrease the core hole shielding, and decrease the relative energy of the optical orbital. In the IVO calculations, the character of the (N − 1)-electron part of the electronic structure is calculated for the (N − 1)-electron core-excited cation, without the effect of the electron in the optical orbital. Therefore, in MO calculations that do not include the electron in the optical orbital, the core hole is overscreened, and the energy of core → valence transitions is systematically overestimated.

We have fit the data in Figure 2 to the formula $E_{exp} = mE_{calc} + b$, and determined a slope of 0.9699 and a y-intercept of 6.4892 (R^2 = 0.9765). In comparison, the corresponding relation

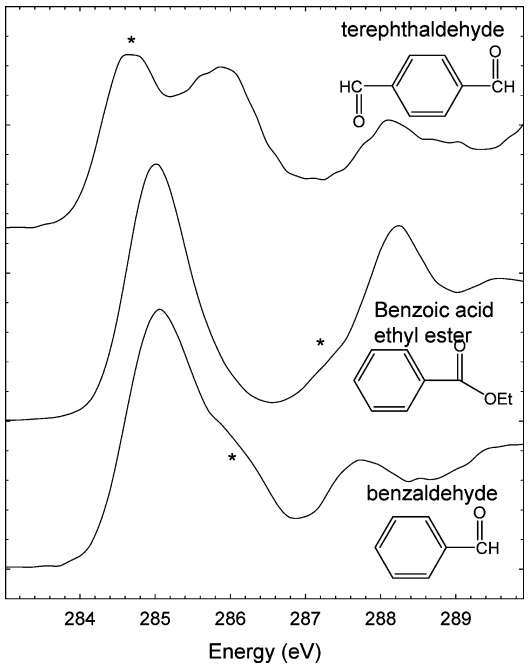

Figure 3. C 1s inner shell electron energy loss spectra of benzaldehyde, ethyl benzoate, and terephthalaldehyde, downloaded from the McMaster Gas-Phase Core Excitation Bibliography.[25,31,32] An asterisk identifies the C 1s (C−R) → $\pi^*_{C=C}$ transitions as originally assigned.

in our previous work on the C 1s(C═O) → $\pi^*_{C=O}$ family of transitions was $E_{exp} = 0.9288E_{calc} + 17.8300$ ($R^2 = 0.9805$).[15] The larger slope calculated for the C 1s (C−R) → $\pi^*_{C=C}$ series relative to the higher energy C 1s (C═O) → $\pi^*_{C=O}$ series demonstrates the energy scale "stretch" commonly observed for MO calculations;[18] higher energy transitions are "more stretched" than lower energy transitions.

In Figure 2, three points, corresponding to benzaldehyde, ethyl benzoate, and terephthalaldehyde, lie outside the otherwise well-defined scatter and were excluded from this semiempirical relation. We believe these absorptions were misassigned in the original reference.[25] The spectroscopic data and original assignments[25] of the benzene C 1s (C−R) → $\pi^*_{C=C}$ transitions are presented in Figure 3.

We can use this semiempirical relation to predict the experimental energy for these C−R transitions, from our calculated transition energies. Using this approach, we predict that the C 1s (C−R) → $\pi^*_{C=C}$ transitions will occur at ∼284.7, 285.0, and 284.4 eV for benzaldehyde, ethyl benzoate, and terephthalaldehyde, respectively. The predicted energy of these C 1s (C−R) → $\pi^*_{C=C}$ transitions will therefore overlap with the C 1s (C−H) → $\pi^*_{C=C}$ transitions and will be unresolved. The original assignments were based on Extended Hückel MO calculations, where the ionization potentials were estimated from literature values for similar molecules. These higher quality ab initio calculations, where the ionization potential is calculated by the ΔSCF method, are a more reliable method for estimating these transition energies.

The original assignments for benzaldehyde, benzoic acid ethyl ester, and terephthalaldehyde were incorrect because the overlap of the "C−R" and "C−H" spectral features was both unexpected and unresolved. These cases indicate an inherent limitation of the C−R shift as an analytic "fingerprint". The utility of the C−R shift depends on it being resolvable—separate from the benzene C 1s (C−H) → $\pi^*_{C=C}$ transitions. To demonstrate the potential for overlap we have compiled a small subset of C−H and C−R data from our ab initio calculations for major substituent types, presented in Table 4. The magnitude of the C−R shift is computed as the energy difference between the C 1s (C−R) → $\pi^*_{C=C}$ transition and the closest of the ortho, meta, and para C 1s (C−H) → $\pi^*_{C=C}$ transitions. When the C 1s (C−R) → $\pi^*_{C=C}$ transition occurs within the C−H band, "no shift" is listed as the C−R shift energy.

TABLE 4: Overlap between Calculated Benzene C 1s (C−H) → $\pi^*_{C=C}$ (ortho, meta, para) and Calculated Benzene C 1s (C−R) → $\pi^*_{C=C}$ Transition Energies

	benzene C 1s → $\pi^*_{C=C}$ transition				
molecule	ortho	meta	para	C−R	C−R shift,[a] eV
benzaldehyde	286.69	287.20	286.76	286.90	no shift
benzoic acid	286.84	287.19	286.81	287.11	no shift
vinylbenzene	286.98	287.34	287.01	287.35	0.01
toluene	287.23	287.23	287.31	287.51	0.20
benzonitrile	286.79	287.14	286.68	287.75	0.61
phenyl urea	287.30	287.29	287.27	288.43	1.13
aniline	287.27	287.32	287.49	289.03	1.54
phenyl acetate	287.35	287.30	287.36	288.97	1.61
phenol	287.17	287.24	287.43	289.23	1.80
fluorobenzene	287.31	287.23	287.36	289.71	2.35

[a] Measured relative to the closest C−H transition.

From these data it is evident that a significant and resolvable C−R shift can be anticipated when the substituent is bonded through an atom or functionality causing a large inductive effect (large IP shift). This observation is consistent even in scenarios such as nitrobenzene, where strong conjugation of valence structure (large term value shift) reduces the magnitude of the C−R shift. When the substituent possesses a moderate inductive influence, such as carbon and carbonyl bound substituents, the degree of conjugation with the benzene π^* density affects its resolvability. For example, toluene, with an sp^3 methyl substituent, has a smaller term value that styrene, so toluene should be expected to produce a C−R absorption shoulder on the higher energy side of the C−H band. In Table 4, this "C−R" shift is predicted to be 0.2 eV. In reality, it will be difficult to resolve such a small shift, as vibronic broadening on the C 1s → π^* bands will have a similar magnitude as the C−R shift[28] and obscure this feature. In situations with pronounced conjugation, such as for sp and sp^2 carbons directly bound to the benzene ring, π-interactions are not likely to allow the C−R transition to be experimentally distinguished from the C−H band. The C 1s (C−R) → $\pi^*_{C=C}$ transition is unlikely to be observed for molecules in which the C−R substituents have a relatively weak inductive effect, coupled with strong conjugation to the benzene ring π^* density.

Another potential complication to the proper assignment of the C−R peak is overlap with a second C 1s(C−H) → $\pi^*_{C=C}$ transition at slightly higher energy than the usual ∼285 eV C 1s(C−H) → $\pi^*_{C=C}$ transition. The second C 1s(C−H) → $\pi^*_{C=C}$ bands that sometimes appear in aromatic molecules can be traced back to the doubly degenerate e_{2u} π^* levels in benzene. In benzene, when a core hole is placed on a carbon atom, the degeneracy of the e_{2u} π^* is lifted, and the lower π^* level is spectroscopically active while the π^* level at higher energy is spectroscopically inactive due to an orbital node on the core excited atom.[18] In some molecules, the π^* orbitals of the substituent can interact with the benzene ring π^* density, causing the higher π^* orbital to be spectroscopically active. C 1s(C−H) → π^* transitions for this higher π^* orbital can overlap with C−R features. The second π^* transition has been most strongly observed for benzene groups that are para substituted by carbonyl-containing groups (e.g., terephthalic acid,[25] dimethyl terephthalate, etc.),[18] but is weak for benzene groups that are

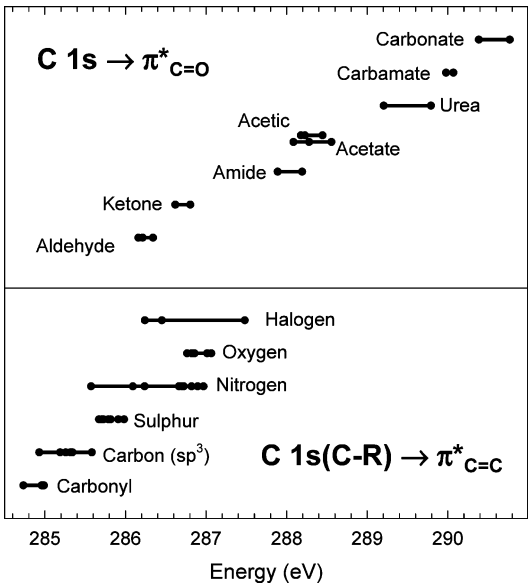

Figure 4. Spectroscopic correlation diagram for (bottom) the C 1s (C−R) → $\pi^*_{C=C}$ transitions and (top) for the carbonyl C 1s (C═O) → $\pi^*_{C=O}$ transitions, reproduced with permission from ref 15, presented on a common energy scale.

singly substituted by carbonyl-containing groups. Simply, one must exercise caution in assigning C−R π^* features in multi-substituted aromatic molecules, as this C−H π^* feature can be strong. This limitation to the analytic utility of the C−R shift is listed so that appropriate caution can be exercised in the use of these features for chemical analysis.

We can accurately predict the energy of a specific transition based on the semiempirical correction of Figure 2. The data displayed in Table 2 and the correction factor have allowed us to construct the *spectroscopic correlation diagram* for the C 1s (C−R) → $\pi^*_{C=C}$ transitions of substituted benzene molecules seen in Figure 4. The correlation diagram for C 1s (C═O) → $\pi^*_{C=O}$ transitions is included in this plot,[15] illustrating the nature and risks of overlapping features in the NEXAFS spectra of organic molecules. For the C−R correlation diagram, bands are grouped by the identity of the primary functionality of the C−R substituent. For the C═O correlation diagram, bands are grouped by the atoms bonded to the C═O group. Individual dots represent individual data points from the calculations, as corrected by the semiempirical factor. The line is an attempt to represent the *range* of each type of C−R band. This is intended to simultaneously represent the power and the limitations of the C−R band as an analytical handle; there are clear chemical shifts, yet potential overlaps with other transitions (π^* C═O; π^* C−H). These correlation diagram lines are prepared from a large dataset, but obviously do not encompass all possible C−R shifts. Therefore, they should be used as guidelines, not absolute delimiters.

The tools used to develop this C−R correlation diagram, specifically the ability to transform calculated transition energies to an "absolute" or experimental energy scale, will be useful in the prediction and assignment of the spectral features of organic compounds. By use of a standard geometry (HG 6-31G* optimization) and basis set (see §2) for spectroscopic calculations, it is possible to predict, with useful accuracy, the energy of a C−R or C═O band for a molecule. This tool should be used with caution: these calculations are only as good as the molecular geometries used for the calculations. Molecules can have a different geometry and conformation in the solid state, and these differences may distort the NEXAFS spectra. This effect will be significant if there are large differences in the π^*-conjugation within the molecule, such as might happen if the relative inclination of the two benzene rings in biphenyl was altered, for example. In contrast, the recent IVO calculations of Gordon et al., on glycyine and glycyl-glycine, show only small differences in peak position and intensity for a variety of expected gas-phase conformations.[29] Another concern is the effect of hydrogen bonding on the condensed state spectra, such as for carboxylic acid dimers. For example, the near-edge structure in the O 1s spectra of water shows remarkable sensitivity to the nature of hydrogen bonding.[30] When using this semiempirical method to predict the energy of a transition, the possible conformations and intramolecular effects should be considered. With appropriate caution, this correction method should be useful for analytical studies of components that are difficult to model experimentally, such as reactive intermediates or side reaction products.

4. Conclusions

We have compiled a set of reliable experimental C 1s NEXAFS or ISEELS spectra of substituted benzene molecules with a wide variety of subtituents. The observed trends of the substituent bonded benzene core C 1s (C−R) → $\pi^*_{C=C}$ transitions have been carefully calibrated and were interpreted with high-quality ab initio calculations, allowing for the development of a reliable semiempirical method of determining the absolute transition energy. Variations in both core binding and valence (π^*) orbital energies were seen to contribute to the observed chemical shifts. With use of this semiempirical method a spectroscopic correlation diagram was developed for the benzene core C 1s (C−R) → $\pi^*_{C=C}$ transitions. We expect this correlation diagram to be useful in guiding chemical identification of organic compounds using NEXAFS spectroscopy. This should make it easier to consider the spectra of species that cannot be easily modeled, and reduce the risk of accidental misidentification of overlapping absorption features.

Acknowledgment. This work was supported by the Natural Science and Engineering Research Council, the Canadian Foundation for Innovation, and the University of Saskatchewan. R.C. is a recipient of an A.C. Nixon summer research fellowship in the University of Saskatchewan Chemistry Department. A. Hitchcock's gas-phase bibliography and Gas Phase Core Excitation database (http://unicorn.mcmaster.ca) has been extremely useful for this study.

References and Notes

(1) Ade, H.; Urquhart, S. NEXAFS spectroscopy and microscopy of natural and synthetic polymers. In *Chemical Applications of Synchrotron Radiation*; Sham, T. K., Ed.; World Scientific Publishing: River Edge, NJ, 2002.

(2) Urquhart, S. G.; Hitchcock, A. P.; Smith, A. P.; Ade, H. W.; Lidy, W.; Rightor, E. G.; Mitchell, G. E. *J. Electron Spectrosc. Relat. Phenom.* **1999**, *100*, 119.

(3) Rightor, E. G.; Urquhart, S. G.; Hitchcock, A. P.; Ade, H.; Smith, A. P.; Mitchell, G. E.; Priester, R. D.; Aneja, A.; Appel, G.; Wilkes, G.; Lidy, W. E. *Macromolecules* **2002**, *35*, 5873.

(4) Mitchell, G. E.; Wilson, L. R.; Dineen, M. T.; Urquhart, S. G.; Hayes, F.; Rightor, E. G.; Hitchcock, A. P.; Ade, H. *Macromolecules* **2002**, *35*, 1336.

(5) Dhez, O.; Ade, H.; Urquhart, S. G. *J. Electron Spectrosc. Relat. Phenom.* **2003**, 85−96.

(6) Stöhr, J. *NEXAFS Spectroscopy*; Springer-Verlag: Berlin, Germany, 1992; Vol. 25.

(7) Kikuma, J.; Tonner, B. P. *J. Electron Spectrosc. Relat. Phenom.* **1996**, *82*, 53.

(8) Morin, C.; Hitchcock, A. P.; Cornelius, R. M.; Brash, J. L.; Urquhart, S. G.; Scholl, A.; Doran, A. *J. Electron Spectrosc. Relat. Phenom.* **2004**, *137*−*140*, 785.

(9) Morin, C.; Ikeura-Sekiguchi, H.; Tyliszczak, T.; Cornelius, R.; Brash, J. L.; Hitchcock, A. P.; Scholl, A.; Nolting, F.; Appel, G.; Winesett, D. A.; Kaznacheyev, K.; Ade, H. *J. Electron Spectrosc. Relat. Phenom.* **2001**, *121*, 203.

(10) Minko, S.; Muller, M.; Usov, D.; Scholl, A.; Froeck, C.; Stamm, M. *Phys. Rev. Lett.* **2002**, *88*, 35502.

(11) *Chemical Applications of Synchrotron Radiation*; Sham, T. K., Ed.; World Scientific Publishing: River Edge, NJ, 2002.

(12) Ratto, F.; Rosei, F.; Locatelli, A.; Cherifi, S.; Fontana, S.; Heun, S.; Szkutnik, P.-D.; Sgarlata, A.; Crescenzi, M. D.; Motta, N. *Appl. Phys. Lett.* **2004**, *84*.

(13) Unger, W. E. S.; Lippitz, A.; Wöll, C.; Heckmann, W. *Fresenius' J. Anal. Chem.* **1997**, *358*, 89.

(14) Ade, H.; Winesett, D. A.; Smith, A. P.; Anders, S.; Stammler, T.; Heske, C.; Slep, D.; Rafailovich, M. H.; Sokolov, J.; Stöhr, J. *Appl. Phys. Lett.* **1998**, *73*, 3775.

(15) Urquhart, S. G.; Ade, H. *J. Phys. Chem. B* **2002**, *106*, 8531.

(16) Urquhart, S. G.; Smith, A. P.; Ade, H. W.; Hitchcock, A. P.; Rightor, E. G.; Lidy, W. *J. Phys. Chem. B* **1999**, *103*, 4603.

(17) Slep, D.; Asselta, J.; Rafailovich, M. H.; Sokolov, J.; Winesett, D. A.; Smith, A. P.; Ade, H.; Strzhemechny, Y.; Schwarz, S. A.; Sauer, B. B. *Langmuir* **1998**, *14*, 4860.

(18) Urquhart, S. G.; Hitchcock, A. P.; Smith, A. P.; Ade, H.; Rightor, E. G. *J. Phys. Chem. B* **1997**, *101*, 2267.

(19) Kosugi, N.; H., K. *Chem. Phys. Lett.* **1980**, *74*, 490.

(20) Hunt, W. J.; Goddard, W. A. I. *Chem. Phys. Lett.* **1969**, *3*, 414.

(21) *Spartan ES 02*; Wavefunction Inc.: Irvine, CA.

(22) Huzinaga, S.; Andzelm, J.; Klobukowski, M.; Radzio-Andzelm, E.; Sasaki, Y.; Tatewaki, H. *Gaussian Basis Sets for Molecular Orbital Calculations*; Elsevier: Amsterdam, The Netherlands, 1984.

(23) Sohdi, R. N. S.; Brion, C. E. *J. Electron Spectrosc. Relat. Phenom.* **1984**, *34*, 363.

(24) Eustatiu, I. G.; Huo, B.; Urquhart, S. G.; Hitchcock, A. P. *J. Electron Spectrosc. Relat. Phenom.* **1998**, *94*, 243.

(25) Hitchcock, A. P.; Urquhart, S. G.; Rightor, E. G. *J. Phys. Chem.* **1992**, *96*, 8736.

(26) Francis, J. T.; Hitchcock, A. P. *J. Phys. Chem.* **1992**, *96*, 6598.

(27) Breitmaier, E.; Voelter, W. *Carbon-13 NMR Spectroscopy*: *high-resolution methods and applications in organic chemistry and biochemistry*, 3rd ed.; VCH: Weinheim, Germany, 1987.

(28) Urquhart, S. G.; Ade, H.; Rafailovich, M.; Sokolov, J. S.; Zhang, Y. *Chem. Phys. Lett.* **2000**, *322*, 412.

(29) Gordon, M. L.; Cooper, G.; Araki, T.; Morin, C.; Turci, C. C.; Kaznatcheev, K.; Hitchcock, A. P. *J. Phys. Chem. A* **2003**, *107*, 6144.

(30) Wernet, P.; Nordlund, D.; Bergmann, U.; Cavalleri, M.; Odelius, M.; Ogasawara, H.; Näslund, L. Å.; Hirsch, T. K.; Ojamäe, L.; Glatzel, P.; Pettersson, L. G. M.; Nilsson, A. *Science* **2004**, *304*, 995.

(31) Hitchcock, A. P.; Mancini, D. C. *J. Electron Spectrosc. Relat. Phenom.* **1994**, *67*, 1.

(32) Hitchcock, A. P.; Mancini, D. C. Gas-Phase Core Excitation Database: http://unicorn.mcmaster.ca/corex/cedb-title.html.

(33) Hitchcock, A. P.; Pocock, M.; Brion, C. E.; Banna, M. S.; Frost, D. C.; McDowell, C. A.; Wallbank, B. *J. Electron Spectrosc. Relat. Phenom.* **1978**, *13*, 2267.

(34) Hitchcock, A. P.; Urquhart, S. G. Unpublished data, 1997.

(35) Nordgren, J.; Glans, P.; Gunnelin, K.; Guo, J.; Skytt, P.; Sathe, C.; Wassdahl, N. *Appl. Phys.* **1997**, *A65*, 97.

(36) Urquhart, S. G.; Hitchcock, A. P. Unpublished data, 1996.

(37) Urquhart, S. G.; Ade, H. W.; Smith, A. P.; Hitchcock, A. P.; Rightor, E. G.; Lidy, W. *J. Phys. Chem. B* **1999**, *103*, 4603.

(38) Urquhart, S. G. Core Excitation Spectroscopy of Molecules and Polymers, Ph.D. Thesis, McMaster University, 1997.